Acta Odontologica Scandinavica, 2013; 71: 72–81

ORIGINAL ARTICLE

Effects of micromovement on the changes in stress distribution of partially stabilized zirconia (PS-ZrO_2) dental implants and bridge during clenching: A three-dimensional finite element analysis

ANDY H. CHOI[1,2], JUKKA MATINLINNA[1] & BESIM BEN-NISSAN[1]

[1]*Dental Materials Science, Faculty of Dentistry, The University of Hong Kong, Hong Kong, PR China, and* [2]*Faculty of Science, University of Technology, Sydney, Australia*

Abstract

Objective. This investigation aims to evaluate the changes in stress magnitudes and distributions on Partially Stabilized Zirconia (PS-ZrO_2) dental implants and bridges and on the mandible caused by fibrous encapsulations during clenching. ***Materials and methods.*** Four 3.26 mm diameter PS-ZrO_2 dental implants with lengths of 12 mm were modelled and placed in the second premolar and first molar region on both sides of the mandible model. A rigid zirconia bridge with a thickness of 0.5 mm connects the PS-ZrO_2 dental implants placed in the second premolar and first molar. Four periodontal ligament (PDL) case studies were examined: PDL in the second premolars; PDL in the first molars; PDL in both the second premolars and first molars; and no PDL present. ***Results.*** The results reveal the magnitudes and distributions of stresses on the dental implants and connecting bridges were governed by the PDLs. A significant drop in stress levels were recorded when the PDL encapsulates the roots of the dental implants. Of the four PDL case studies, it was found that when the PDLs are present in both the second premolars and first molars the lowest stress magnitudes are generated. The analysis also revealed that, during the healing process after implant insertion and the result of fibrous encapsulation, the dental implant system will experience a varying amount of stress levels. ***Conclusion.*** This study was intended to produce more insight into the influence of the PDL on the changes in stress distribution on the dental implant system during clenching.

Key Words: *finite element analysis, FEA, mandible, zirconia implant, periodontal ligament, fibrous encapsulation, PDL, PS-*ZrO_2

Introduction

Implants are the nearest equivalent replacement to the natural tooth and are, therefore, a useful addition in the management of patients who have missing teeth because of disease, trauma or developmental anomalies. There are a number of dental implant systems which offer predictable long-term results backed by good scientific research and clinical trials. It is important to establish success criteria for implant systems and for implants to be tested in well-controlled clinical trials.

The most obvious sign of implant failure is mobility and its influence on the surrounding bone [1]. The stability of the implant at the time of placement is very important and is dependent upon bone quantity and quality as well as implant design. Following loss of a tooth, the alveolar bone resorbs in width and height. The most favourable quality of jawbone for implant treatment is that which has a well-formed cortex and densely trabeculated medullary spaces with a good blood supply. Bone which is predominately cortical may offer good initial stability at implant placement but is more easily damaged by overheating during the drilling process, especially with sites more than 10 mm in depth. At the other extreme, bone with a thin or absent cortical layer and sparse trabeculation offers very poor initial implant stability and fewer cells with good osteogenic potential to promote osseointegration.

Following installation of an implant it is important that it is not excessively loaded during the early healing phase. This has been compared to the healing of a fracture where stabilization of the bone fragments is very important to promote union. Movement of the implant within the bone at this stage results in fibrous

Correspondence: Dr Andy H. Choi, Dental Materials Science, Faculty of Dentistry, University of Hong Kong, Hong Kong. E-mail: ahchoi@hotmail.com

(Received 3 May 2011; accepted 14 December 2011)

ISSN 0001-6357 print/ISSN 1502-3850 online
DOI: 10.3109/00016357.2011.654242

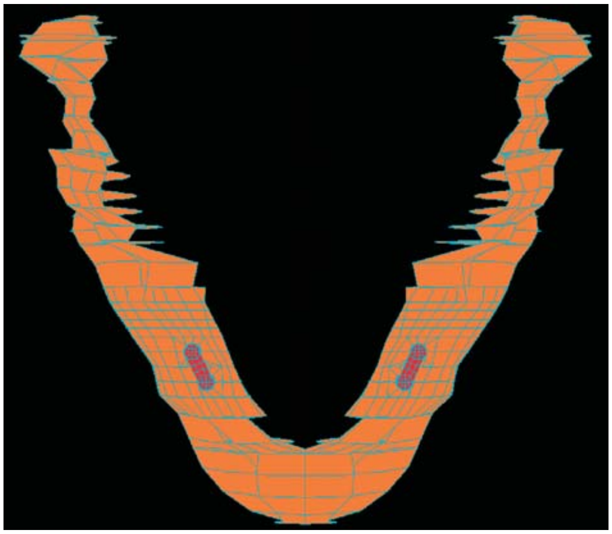

Figure 1. Top view of the finite element model of the human mandible with the insertion of PS-ZrO$_2$ dental implants and bridges (produced in Strand7).

tissue encapsulation rather than osseointegration. Studies revealed that a capsule of fibrous tissue was found around the implants that were not kept immobile during the healing process [2].

During the initial loading, the more stable the implant is, the less micromovement there will be, and this in turn will lead to higher rates of success [3–5]. Studies in the past have revealed implants that have micromovement as a result of axial, tensile or compression forces may still undergo osseointegration. Various investigators [6,7] have discovered that micromotions less than 150–200 μm will not lead to failure of the osseointegration, while a maximum limit of 150 μm has been reported in the literature for micromotion to ensure the success of implants [8–10].

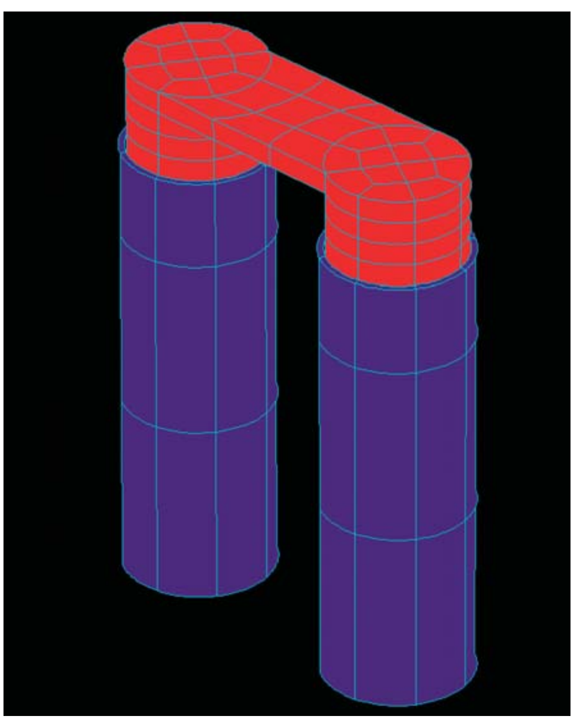

Figure 2. Schematic showing the basic layout of the PS-ZrO$_2$ dental implants and the connecting bridge (red) and the encapsulating periodontal ligament (blue) (produced in Strand7).

Carefully planned functional occlusal loading will result in maintenance of osseointegration and possibly increased bone-to-implant contact. In contrast, excessive loading or not enough load transfer may lead to bone loss and/or component failure.

Finite element analysis has long served as a method to study the primary stability of implants and stress distribution in their surrounding bone.

The effects of cortical bone thickness and implant length on strain in the surrounding bone and micromotion at the bone–implant interface in single immediately loaded implants were investigated by Tu et al. [11]. A series of computed tomography images of a posterior mandible of a dry human skull were obtained from the premolar to the first molar. Vertical and lateral loads of 130 N were applied to the models.

Fazel et al. [12] assessed and compared peri-implant stress distribution and micromotion of two types of immediate loading implants using finite element analysis. Accurate pictures of two fixtures were taken by a digital camera. Following accurate measurements, the three-dimensional finite element computer model was simulated. In order to make a model of a mandible, moulding was done on a toothless patient and then a plaster model was prepared. Two-millimetre sections of this plaster model were prepared and, using their measures that were transferred to the computer, the model of a mandibular bone was prepared. In this model, the thickness of the cortical bone was 2 mm and the rest of the model was filled with spongy bone. A loading of 500 N with an angle of 75° with horizon was applied to the model.

The finite element models used in most of these studies have been almost exclusively first-order, partially complete mandibular models, some exhibiting limited anatomic description and properties. Improvements implemented with this current model include forces acting on the mandible, realistic geometry and boundary conditions analogous to musculature support and ultimately better bone and tissue property characterization, both structurally and biologically.

Zirconia has recently been introduced as a dental implant fixture material. However, theoretical evaluations about its durability are still inadequate [13,14]. Therefore, the aim of this investigation is to evaluate the changes in stress magnitudes and distributions on Partially Stabilized Zirconia (PS-ZrO$_2$) dental implants and bridges and on the mandible caused by fibrous encapsulations during clenching using an anatomically accurate three-dimensional finite element mandibular model. This study also aims to determine whether these changes are sufficient to jeopardize the longevity of the implants and bridges.

Table I. Mechanical properties used in finite element analysis [17-24].

	Young's modulus (GPa)			Poisson's ratio			Tensile strength	Compressive strength
	E_1	E_2	E_3	ν_{12}	ν_{23}	ν_{13}	(MPa)	(MPa)
Cortical bone	6.9	8.2	17.3	0.315	0.325	0.310	121–135	167–205
Cancellous bone	0.32	0.39	0.96	0.3	0.3	0.3		
PS-ZrO2	210			0.31			800–1500	1990
Periodontal ligament	0.0689			0.45				

Materials and methods

Mandible model

A dry human mandible has been used to define the geometry of the model. Finite element analyses were carried out under non-linear static conditions. Both the modelling and analysis were performed with a commercially available finite element analysis package, STRAND7 (G + D Computing, Sydney, Australia). For this analysis three nodes on the symmetry plane were fixed in space by the use of spring elements. The model is completely free to deform, removing the approximation caused by over-restraining the model [15,16].

Dental implants and bridges

Four Partially Stabilized Zirconia (PS-ZrO_2) dental implants with a diameter of 3.26 mm were modelled as cylindrical solid structures with abutments that were 2 mm high. The depth of the implant–cortical interface varies from location to location on the mandible model. For this study, the implant was placed in the second premolar and first molar region on sides of the mandible model and has a depth of 2 mm.

Implant lengths of 12 mm with a depth of penetration into the cancellous bone of 8 mm were modelled. A rigid PS-ZrO_2 bridge with a thickness of 0.5 mm was modelled as a solid structure connecting the dental implants placed at the second premolar and first molar (Figure 1).

Four PDL case studies were examined:

- PDL in the second premolars ($PDL_{premolars}$);
- PDL in the first molars (PDL_{molars});
- PDLs in both the second premolars and first molars ($PDL_{premolars + molars}$); and
- No PDL present ($PDL_{reference}$).

The tensile and compressive stresses obtained from $PDL_{reference}$ will be used as a reference to measure the percentage change caused by various kinds of micromotion.

Periodontal ligaments

The periodontal ligament (PDL), which plays the most significant role in tooth mobility, is a soft, richly vascular and cellular connective tissue that surrounds the roots of the teeth and joins the root cementum with the alveolar bone proper [10].

In this study, a layer of PDL, modelled as a linear-elastic solid structure with a uniform thickness of 0.26 mm, surrounds and encapsulates the roots of the dental implants (Figure 2).

Material properties and muscle forces

All the materials in this model were assumed to be isotropic, homogeneous and linearly elastic. The mechanical properties of cortical and cancellous bone and the periodontal ligament were selected from various investigators. The mechanical properties

Table II. Calculated muscle, joint reaction and bite force magnitudes (N) acting on the mandible during clenching [15,16].

Muscles	Force (N)
Bite Force (2nd premolar)	246.3
Bite Force (1st molar)	157.4
Joint Reaction Force	471.9
Lateral Pterygoid	378.0
Masseter	340.0
Medial Pterygoid	191.4
Openers	155.0
Temporalis^{Anterior}	264.3
Temporalis^{Posterior}	264.3

Table III. The maximum tensile stress (MPa) recorded on the PS-ZrO_2 dental implants and bridge during various PDL case studies.

	2nd premolars	1st molars	Bridge
$PDL_{premolars}$	*19.50*	50.69	66.55
PDL_{molars}	42.96	*15.34*	55.70
$PDL_{premolars + molars}$	*14.28*	*17.92*	21.78
$PDL_{reference}$	35.99	45.17	56.95

Italicized values represent location(s) of the PDL(s) during each case study.

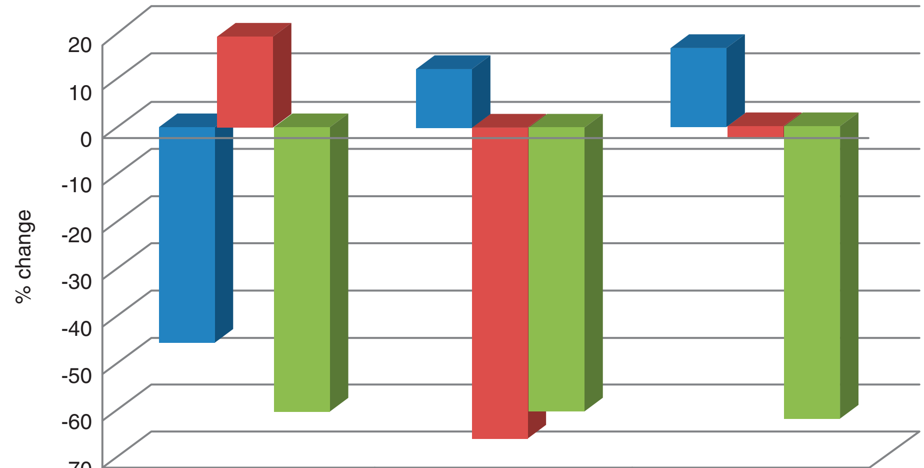

	2nd premolar	1st molar	Bridge
PDLpremolars	-45.82	12.22	16.86
PDLmolars	19.37	-66.04	-2.19
PDLpremolars+molars	-60.32	-66.33	-61.76

Figure 3. Percentage change in maximum tensile stress recorded on the PS-ZrO$_2$ dental implants and bridge during various PDL case studies.

of cortical and cancellous bone, PDL and PS-ZrO$_2$, are given in Table I [17–24].

The muscle forces considered in this analysis were selected from various investigators [25–28]. All the forces were assumed to be symmetrical with respect to the mid-line and to have an equal magnitude on the right and left side of the mandible. The forces exerted by contracting muscles were represented by

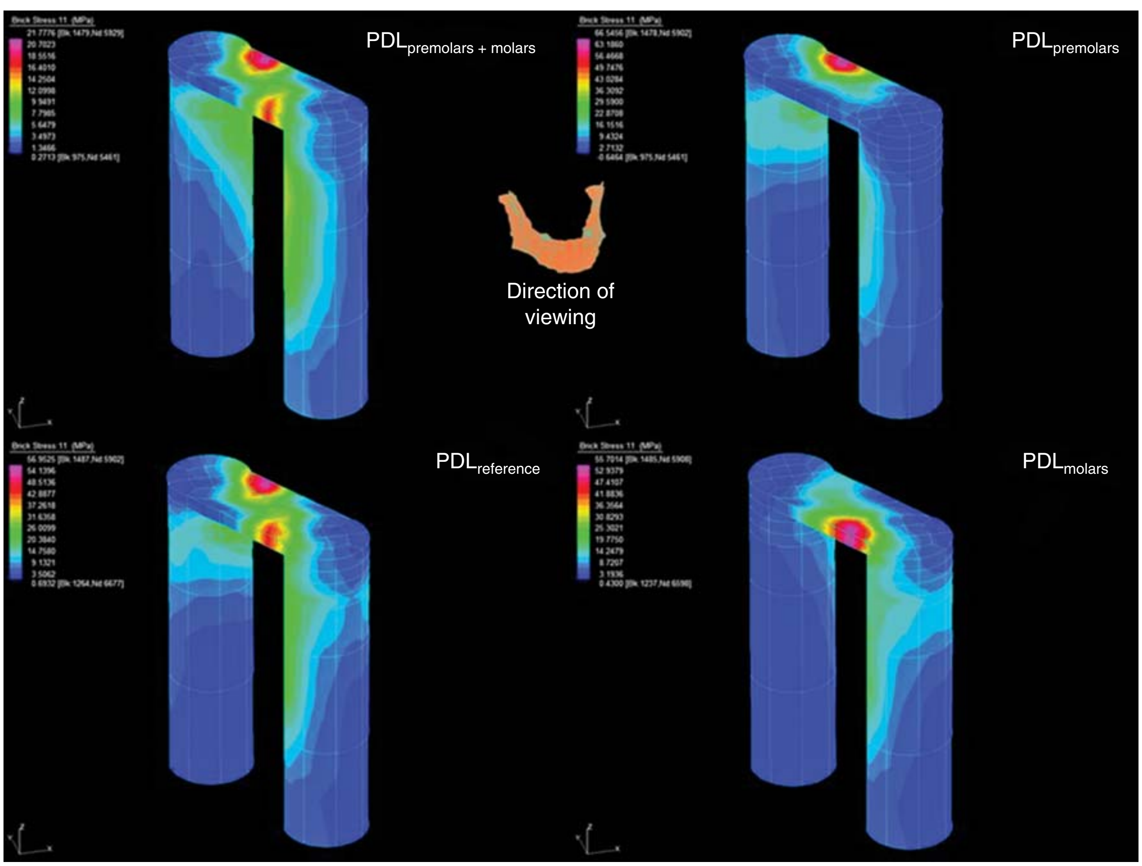

Figure 4. Contour plots of the tensile stress recorded on the PS-ZrO$_2$ dental implants and connecting bridges during different PDL case studies.

Table IV. Maximum tensile stress (MPa) recorded on the mandible during various PDL case studies.

	Maximum Tensile Stress (MPa)
$PDL_{premolars}$	27.75
PDL_{molars}	27.75
$PDL_{premolars\ +\ molars}$	27.75
$PDL_{reference}$	27.76
No implant	27.24

vectors. For this present work, the bite force (clench force) was directed at an angle of ~ 85° to the averaged occlusal plane. Each bite force was equally divided between two teeth symmetrically placed with respect to the midsagittal plane [15,16].

During clenching all muscles were assumed to be active. Calculated muscle forces are given in Table II. The reaction forces were assumed to be acting at the centre of the condyles [15,16].

Results

The maximum principal (tensile), minimum principal (compressive) and Von Mises stresses of the PS-ZrO_2 dental implants and bridge as well as on the overall mandibular model have been analysed under non-linear static conditions using the STRAND7 finite element analysis package. As stated in the methods section, four different PDL case studies were analysed.

The distribution of stresses is shown in the form of contoured colour plots where each colour represents a different value. There are no explicit guidelines in the literature for interpreting the results of stress analysis; principal stresses and Von Mises stress have been used equally. Principal stresses (tensile stress and compressive stress) values are important for brittle materials such as PS-ZrO_2, because failure occurs when tensile stress is greater than or equal to the ultimate tensile strength of bone, or when the compressive stress is greater than or equal to the ultimate compressive strength of PS-ZrO_2. The ultimate stress of bone varies with direction and location as well as from person to person. The ultimate tensile stress of human cortical bone ranged from 121–135 MPa and the ultimate compressive stress ranged from 167–205 MPa. The strength of cancellous bone is much less than that of the cortical bone. Ultimate stress values of cancellous bone vary between 1–20 MPa [23,24].

Table V. The maximum compressive stress (MPa) recorded on the PS-ZrO_2 dental implants and bridge during various PDL case studies.

	2nd premolars	1st molars	Bridge
$PDL_{premolars}$	*25.96*	73.16	93.39
PDL_{molars}	48.99	*17.13*	62.39
$PDL_{premolars\ +\ molars}$	*26.43*	*25.46*	33.18
$PDL_{reference}$	52.50	60.97	76.02

Italicized values represent location(s) of the PDL(s) during each case study.

Von Mises stress values are defined as the beginning of deformation for ductile materials, since failure occurs when Von Mises stress values exceed the yield strength of a material. The Von Mises stress is calculated from the six stress components normally present in three-dimensional stress analysis of homogeneous structures. The structure is safe when the Von Mises stress is less than or equal to the absolute value of the yield stress in tension or compression, as determined in a uniaxial tension of compression test on a sample of the same material.

Maximum principal stress (tensile)

The maximum tensile stresses recorded on the PS-ZrO_2 dental implants inserted into the second premolar and first molar as well as the bridge connecting the dental implants are given in Table III.

When different PDL case studies were analysed, the results reveal a significant drop in the tensile stress values recorded on the PS-ZrO_2 dental implants when a layer of PDL is present. A decrease of 45–66% in the tensile stress (compared to $PDL_{reference}$) was observed on the PS-ZrO_2 dental implants in the second premolars and first molars (Figure 3).

The tensile stress analysis also revealed that the PDLpremolars + molars case study produced the lowest magnitude of tensile stress on both the dental implants and in the bridge connecting the implants.

The contour plots of tensile stress recorded on the PS-ZrO_2 dental implants inserted into the second premolars and first molars as well as the bridge connecting the dental implants during different PDL case studies are shown in Figure 4. The plots reveal the PDLs play a significant role in where the tensile stresses act on the dental implants and bridges during clenching. When the PDL occurs in the second premolars, the tensile stress is most evident on the lingual side of the structure ($PDL_{premolars}$). On the other hand, the tensile stress is most evident on the buccal side of the structure when the PDL occurs on the first molar (PDL_{molars}).

The maximum tensile stress recorded on the mandible with and without the inclusion of PS-ZrO_2 dental implants and bridge is shown in Table IV. The result indicates the maximum tensile stress observed on the mandible remained unchanged when different PDL case studies were analyzed. When these values are compared with the tensile stress recorded on the mandible without the inclusion

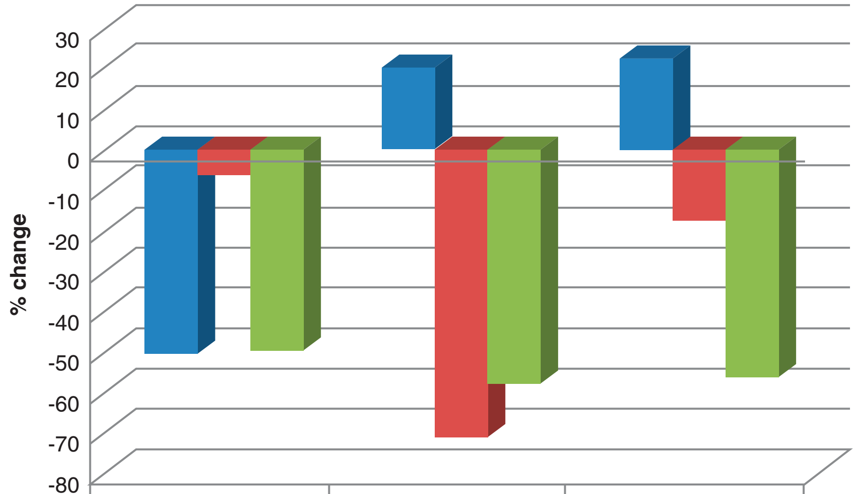

	2nd premolar	1st molar	Bridge
PDLpremolars	-50.55	19.99	22.85
PDLmolars	-6.69	-71.9	-17.93
PDLpremolars + molars	-49.66	-58.24	-56.35

Figure 5. Percentage change in maximum compressive stress recorded on the PS-ZrO_2 dental implants and bridge during various PDL case studies.

of PS-ZrO_2 dental implants, the result indicates there is no change in the tensile stress recorded on the mandible with the inclusion of PS-ZrO_2 dental implants.

Minimum principal stress (compressive)

The maximum compressive stress recorded on the PS-ZrO_2 dental implants inserted into the second

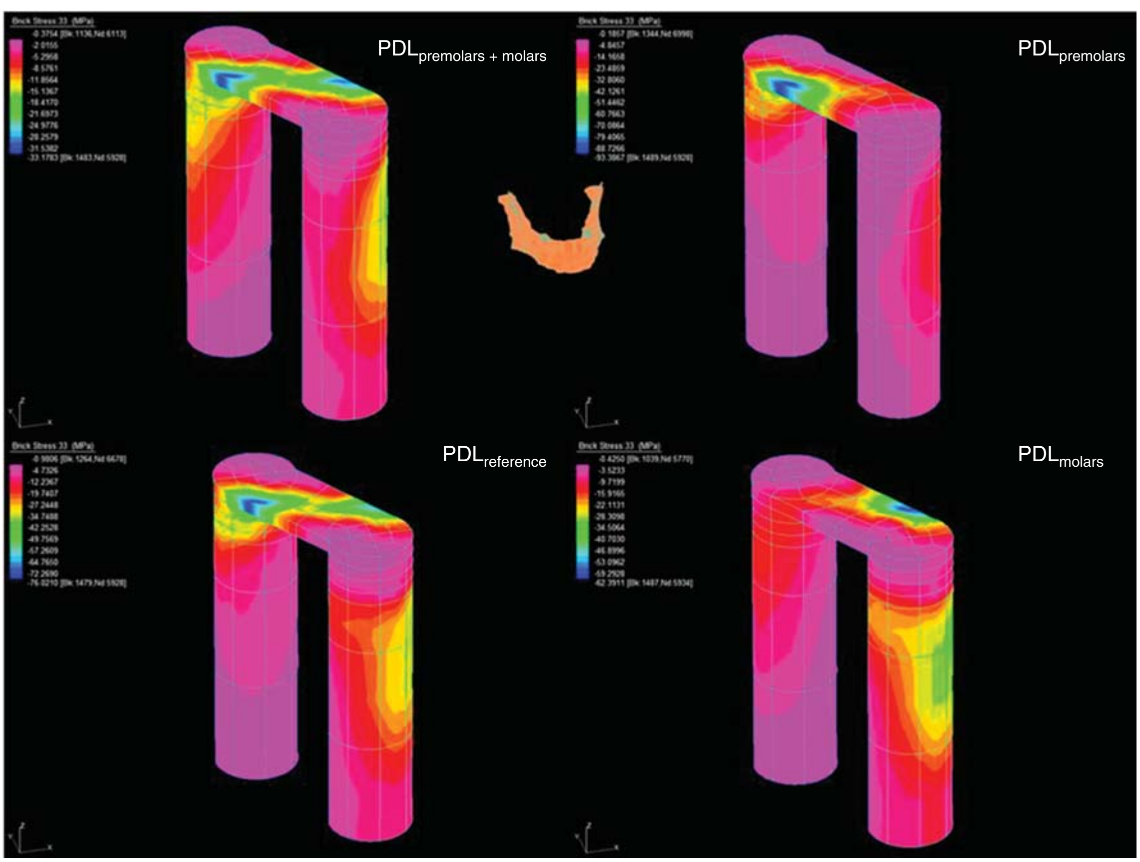

Figure 6. Contour plots of the compressive stress recorded on the PS-ZrO_2 dental implants and connecting bridges during different PDL case studies.

Table VI. Maximum compressive stress (MPa) recorded on the mandible during various PDL case studies.

	Maximum Compressive Stress (MPa)
$PDL_{premolars}$	36.26
PDL_{molars}	36.26
$PDL_{premolars + molars}$	36.26
$PDL_{reference}$	36.26
No implant	36.23

premolar and first molar as well as the bridge connecting the dental implants are given in Table V.

Similar to the tensile stress analysis, when different PDL case studies were studied the results reveal a significant drop in the compressive stress values recorded on the PS-ZrO_2 dental implants when a layer of PDL is present. A decrease of 50–60% in the compressive stress was observed on the PS-ZrO_2 dental implants in the second premolars and first molars.

The compressive stress analysis again reveals that the PDLpremolars + molars case study generated the lowest magnitude of compressive stress on both the dental implants and in the bridge connecting the implants (Figure 5).

The contour plots of compressive stress recorded on the PS-ZrO_2 dental implants inserted into the second premolars and first molars as well as the bridge connecting the dental implants during different PDL case studies are shown in Figure 6. The contour plots again show PDL plays a significant role in governing the magnitude and locations of compressive stresses observed on the dental implants and bridges.

When the PDL occurs in the second premolars, the compressive stress is most evident on the buccal side of the structure ($PDL_{premolars}$). On the other hand, the compressive stress is most evident on the lingual side of the structure when the PDL occurs on the first molar (PDL_{molars}).

The maximum compressive stress recorded on the mandible with the inclusion of PS-ZrO_2 dental implants and bridge during clenching is shown in Table VI. Similar to tensile stress analysis, the result indicates the maximum compressive stress observed on the mandible remained unchanged when different PDL case studies were analysed. When these values are compared with the compressive stress recorded on the mandible without the inclusion of PS-ZrO_2 dental implants, the result indicates there is no change in the compressive stress recorded on the mandible with the inclusion of PS-ZrO_2 dental implants.

Table VII. The maximum Von Mises stress (MPa) recorded on the PS-ZrO_2 dental implants and bridge during various PDL case studies.

	2nd premolars	1st molars	Bridge
$PDL_{premolars}$	*34.48*	73.34	93.94
PDL_{molars}	49.77	*28.12*	62.97
$PDL_{premolars + molars}$	*26.83*	*25.92*	33.20
$PDL_{reference}$	53.72	61.70	76.84

Italicized values represent location(s) of the PDL(s) during each case study.

Von Mises stress

The maximum Von Mises stress recorded on the PS-ZrO_2 dental implants inserted into the second premolar and first molar as well as the bridge connecting the dental implants are given in Table VII.

Similar to the tensile and compressive stress analyses, when different PDL case studies were studied the results reveal a significant drop in the Von Mises stress values recorded on the PS-ZrO_2 dental implants when a layer of PDL is present. A decrease of 35–60% in the Von Mises stress was observed on the PS-ZrO_2 dental implants in the second premolars and first molars (Figure 7).

The Von Mises stress analysis also revealed that the PDLpremolars + molars case study produced the lowest magnitude of Von Mises stress on both the dental implants and in the bridge connecting the implants.

The contour plots of Von Mises stress recorded on the PS-ZrO_2 dental implants inserted into the second premolars and first molars as well as the bridge connecting the dental implants during different PDL case studies are shown in Figure 8. The contour plots again show PDL plays a significant role in governing the magnitude and locations of compressive stresses observed on the dental implants and bridges.

When the PDL occurs in the second premolars, the Von Mises stress is most evident on the buccal side of the structure ($PDL_{premolars}$). On the other hand, the Von Mises stress is most evident on both the buccal and lingual side of the structure when the PDL occurs on the first molar (PDL_{molars}).

The maximum Von Mises stress recorded on the mandible with and without the inclusion of PS-ZrO_2 dental implants and bridge is shown in Table VIII. Slightly higher Von Mises stress values were recording during PDL_{molars} and $PDL_{reference}$ case studies.

Discussion

The study is aimed at determining the changes in stress magnitudes on the dental implants and bridge caused by micromotion as a result of fibrous encapsulation (periodontal ligament) during functional loading using three-dimensional finite element analysis.

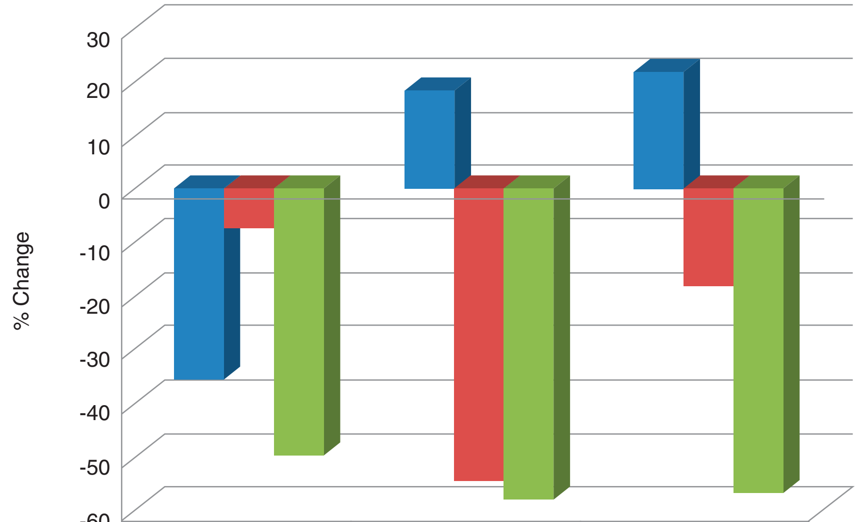

	2nd premolar	1st molar	Bridge
PDLpremolars	-35.82	18.87	22.25
PDLmolars	-7.35	-54.52	-18.05
PDLpremolars+molars	-50.06	-57.99	-56-79

Figure 7. Percentage change in maximum Von Mises stress recorded on the PS-ZrO$_2$ dental implants and bridge during various PDL case studies.

It is almost impossible in terms of a clinical perspective to introduce devices such as strain gauges into the bone–implant interface in an effort to study and evaluate the amount of micromotion under functional loadings such as during mastication. As a result, finite element analysis is ideal for evaluating not only micromovement but the changes in stress distribution patterns during the healing period.

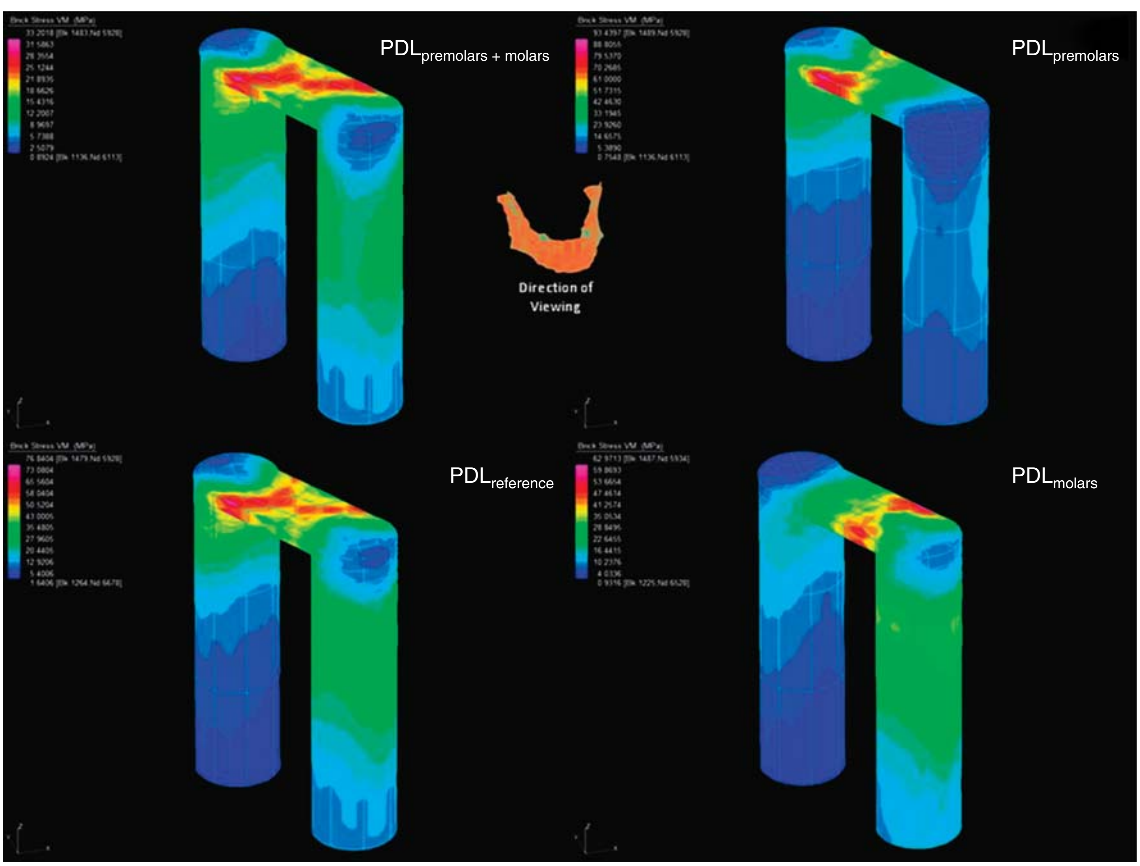

Figure 8. Contour plots of the Von Mises stress recorded on the PS-ZrO$_2$ dental implants and connecting bridges during different PDL case studies.

Table VIII. Maximum Von Mises stress (MPa) recorded on the mandible with the inclusion of PS-ZrO_2 dental implants and bridge.

	Maximum Von Mises Stress (MPa)
$PDL_{premolars}$	39.13
PDL_{molars}	45.87
$PDL_{premolars + molars}$	39.13
$PDL_{reference}$	44.61
No implant	38.91

The finite element method is used to precisely calculate local stress–strain distributions in geometrically complex structures. The predictive accuracy of the finite element model is influenced by the geometric detail of the object to be modelled, the material properties and the applied boundary conditions. Finite element analysis has become widely used in all biomechanical fields, especially for assessing stresses and strains in dental implants and the surrounding bone structures as well as in normal bone.

Due to the presence of the PDL, masticatory loads produced during clenching can be absorbed or distributed into the alveolar bone. The responses of PDL to functional loading are critical to the understanding of the tooth-support mechanism. Hence, determining the direction, magnitude and nature of masticatory loads dissipated by the PDL is extremely important to the understanding of the biologic behaviour of the attachment apparatus under normal and diseased conditions [29].

In this present study it is clearly evident that some of the masticatory loads during clenching have been absorbed by the PDL. As seen in Figures 3, 5 and 7, depending on the location of the PDL, a significant drop in the tensile, compressive and Von Mises stresses were recorded on the PS-ZrO_2 dental implants.

This can be attributed to the fact that the mechanical properties of the PDL (Young's Modulus and Poisson's ratio) are much lower than that of the PS-ZrO_2 as well as the cortical and cancellous bone. Hence, it can be more easily altered and absorb some of the tensile and compressive stress generated by the masticatory forces during clenching. The most significant decrease in the maximum tensile and compressive stresses occurs when the PDL is present in both the second molar and first molar (PDLpremolar + molar).

Although the recorded maximum tensile and compressive stresses on the PS-ZrO_2 may not be significant since its ultimate tensile and compressive strength is far greater that the stress levels experienced during clenching.

This investigation also reveals that although high levels of stresses were recorded on the PS-ZrO_2 dental implants and bridges, the stresses recorded on the mandible with the inclusion of dental implants and bridges and various PDL conditions show that they have no effect on the magnitude of the tensile, compressive and Von Mises stresses during clenching.

During the healing phase after the insertion of dental implants, changes in the magnitude and distribution of stresses observed on the dental implant system is expected as the results of this investigation reveal. It is imperative, both from the dental materials and clinical perspective, that these stress magnitudes are not high and harmful enough to jeopardize the longevity of the dental implant systems.

During functional loadings such as clenching, the dental implant and prosthesis could be subjected to an alternating load oscillating through zero. The result is micromovements between the implant and the bone, this result in fibrous encapsulation instead of osseointegration. This micromovement causes an increase in loosening of the implant. This condition and subsequent fibrosis greatly facilitates infection.

This study was intended to produce more insight into the influence of the PDL on the changes in stress distribution on the dental implant system during clenching. By using the finite element analysis, prediction and calculation of changes in stress distribution within the dental implant systems and the PDL is now made possible.

Conclusion

More insight and understanding into the influence of PDLs during functional movement on the changes in stress distributions on the dental implant system has been obtained using finite element analysis. Furthermore, understanding the changes in the distribution and magnitude of stresses generated in the dental implant system during the healing phase caused by fibrous encapsulation instead of osseointegration could result in better implant design and materials selections.

Acknowledgement

The corresponding author would like to express his gratitude to Endeavour Australia Cheung Kong Research Fellowship (#1988_2011) for supporting this research.

Declaration of interest: The authors report no conflicts of interest. The authors alone are responsible for the content and writing of the paper.

References

[1] Albrektsson T, Zarb G, Worthington P, Eriksson RA. The long-term efficacy of currently used dental implants: a review and proposed criteria of success. Int J Oral Maxillofac Implants 1986;1:11–25.

[2] Donath K, Laass M, Gunzl HJ. The histopathology of different foreigh-body reactions to oral soft tissue and bone tissue. Virchows Archiv Pathol Anat 1992;420:131–7.

[3] Cooper L, Felton DA, Kugelberg CF, Ellner S, Chaffee N, Molina AL, et al. A multicenter 12-month evaluation of single-tooth implants restoration 3 weeks after 1-stage surgery. Int J Oral Maxillofac Implants 2001;16:182.
[4] Fazel A, Aalai S, Rismanchian M. Effect of macro-design of immediately loaded implants on micromotion and stress distribution in surrounding bone using finite element analysis. Implant Dent 2009;18:345.
[5] Brochu J, Anderson J, Zarb G. The influence of early loading on bony crest height and stability: a pilot study. Int J Prosthodont 2005;18:506.
[6] Pilliar RM, Lee JM, Maniatopoulos C. Observations on the effect of movement on bone ingrowth into porous-surfaced implants. Clin Orthop Relat Res 1986;5:108–13.
[7] Viceconti M, Muccini R, Bernakiewicz M, Baleani M, Cristofolini L. Large sliding contact elements accurately predict levels of bone-implant micromotion relevant to osseointegration. J Biomech 2000;33:1611–18.
[8] Brunski JB. Avoid pitfalls overloading and micromotion of intraosseous implants. Dent Implantol Update 1993;4:77–81.
[9] Chong W, Davliakos JP, Fischman B, et al. Immediate loading. Implant Dent 2002;11:315–23.
[10] Lindhe J, Lang NP, Karring T. Clinical periodontology and implant dentistry. Oxford: Blackwell Publishing; 2003. p 279–95.
[11] Tu MG, Hsu JT, Fuh LJ, Lin DJ, Huang HL. Effects of cortical bone thickness and implant length on bone strain and interfacial micromotion in an immediately loaded implant. Int J Oral Maxillofac Implants 2010;25:706–14.
[12] Fazel A, Aalai S, Rismanchian M, Sadr-Eshkevari P. Micromotion and stress distribution of immediate loaded implants: a finite element analysis. Clin Implant Dent Relat Res 2009; 11:267–71.
[13] Ho GW, Matinlinna JP. Insights on porcelain as a dental material. Part I: ceramic material types in dentistry. Silicon 2011;in press; DOI: 10.1007/s12633–011–9079–6.
[14] Liu D, Matinlinna JP, Pow EHN. Insights into porcelain zirconia bonding. J Adhes Sci Techn 2011; submitted 2011.
[15] Choi AH, Ben-Nissan B, Conway RC. Three-dimensional modelling and finite element analysis of the human mandible during clenching. Aust Dent J 2005;50:42–8.
[16] Choi AH, Matinlinna JP, Ben-Nissan B. Finite element stress analysis of Ti-6Al-4V and partially stabilized zirconia dental implant during clenching. Acta Odont Scand 2011; Early Online, 1–9.
[17] Arendts FJ, Sigolotto C. Standard measurements, elastic values and tensile strength behavior of the human mandible, a contribution to the biomechanics of the mandible - I. Biomed Tech 1989;34:248–55.
[18] Arendts FJ, Sigolotto C. Mechanical characteristics of the human mandible and study of in vivo behavior of compact bone tissue, a contribution to the description of biomechanics of the mandible - II. Biomed Tech 1990;35:123–30.
[19] Weinstein AM, Klawitter JJ, Cook SD. Implant-bone interface characteristics of bioglass dental implants. J Biomed Mater Res 1980;14:23–9.
[20] Cook SD, Weinstein AM, Klawitter JJ. Parameters affecting the stress distribution around LTI carbon and aluminium oxide dental implants. J Biomed Mater Res 1982;16:875–85.
[21] Piconi C, Maccauro G. Zirconia as a ceramic biomaterial. Biomaterials 1999;20:1–25.
[22] Callister WD. Materials in science and engineering - an introduction. 7th ed. New York: Wiley & Sons; 2007.
[23] Reilly SB, Burstein AH. The elastic and ultimate properties of compact bone tissue. J Biomech 1975;8:393–405.
[24] Akca K, Iplikcipglu H. Finite element stress analysis of the influence of staggered versus straight placement of dental implants. Int J Oral Maxillofac Implants 2001;16:722–30.
[25] Mainland D, Hiltz EJ. Forces exerted on the human mandible by the muscles of mastication. J Dent Res 1934;14:107–24.
[26] Barbenel JC. The biomechanics of the temporomandibular joint: a theoretical study. J Biomech 1972;5:251–6.
[27] Schumacher GH. Funktionelle morphologie der kinnmuskulatur. Jena: Fisher; 1961.
[28] Pruim GJ, De Jongh HJ, Ten Bosch JJ. Forces acting on the mandible during bilateral static bite at different bite force levels. J Biomech 1980;13:755–63.
[29] Poiate IA, de Vasconcellos AB, de Santana RB, Poiate E. Three-dimensional stress distribution in the human periodontal ligament in masticatory, parafunctional, and trauma loads: finite element analysis. J Periodontol 2009;80: 1859–67.